

# Variations of surface roughness for deposition of Co-sputtered-ZnO(002) by Auger electron spectroscopy and surface magneto-optic Faraday effect

Y.-C. Chang<sup>1</sup>, C.-W. Su<sup>1,a</sup>, S.-C. Chang<sup>1</sup>, and Y.-H. Lee<sup>2</sup>

<sup>1</sup> Department of Electrophysics, National Chiayi University, 60004 Chiayi, Taiwan

<sup>2</sup> Department of Physics, National Cheng Kung University, 1 University Rd., 70101 Tainan, Taiwan

Received: 12 August 2010 / Accepted: 29 November 2010

Published online: 28 January 2011 – © EDP Sciences

**Abstract.** Auger electron spectroscopy and the surface magneto-optical Faraday effect were used to monitor the deposition of Co ultrathin films on an initially rough ZnO(002) crystal surface. The magnetic properties of the epitaxial films were compared with those associated with that the structure properties in a 3D island growth mode. The magneto-optic signals are very sensitive to the thickness of the Co film structure, even if it is rough. The ZnO(002) substrate surface formed by routine ion sputtering may exhibit short-range ordering in the initial sample preparation. The roughness of a sputtered substrate surface can be determined from the sensitive magneto-optical signals, especially when ultrathin films are deposited in the initial stage of growth.

## 1 Introduction

In the last two decades, extensive research has been performed on magnetic metal films on flat and sputtered surfaces, exploiting the surface magneto-optical effect. This approach, which offers convenience of measurement, ease of set-up, non-contact optical detection in a ultrahigh vacuum system, and atomic sensitivity, is a powerful technique for researching ultrathin magnetic films. Co films typically have a strong perpendicular easy axis of magnetisation in the initially grown layer [1–3]. However, Co that is deposited on a semiconductor surface usually exhibits weak magnetism [4,5]. Since the first discovery of a room-temperature ferromagnetism material, Co-doped anatase TiO<sub>2</sub>, oxide-based diluted magnetic semiconductors (DMS) have attracted much interest in the field of spintronics research [6–8]. The growth of magnetic film on a semiconductor surface makes the structure-sensitive magnetic property of the ferromagnetic constituents predictable [9]. In this study, the ZnO(002) crystal surface was adopted as the substrate. ZnO is a well-known wide-band-gap semiconductor material. Its optimum transmittance exceeds 99% under visible light. Therefore, the transmitted probing technique such as magneto-optical Faraday effect is effective for investigating the surface magnetic properties of Co ultrathin films during the growth, especially for the transparent ZnO(002) crystal. The thickness of the deposited Co was estimated from the ratio of the measured Auger intensities of the signals and calculated from the electron inelastic-mean-free-path

database. The roughness of the initial substrate surface was analysed by comparing the magneto-optical signals and the growth, even when the surface was preferentially sputtered by plasma.

## 2 Experiments

All measurements were made in an ultrahigh vacuum (UHV) chamber at a base pressure of  $3 \times 10^{-10}$  Torr. The chamber was equipped with a low energy electron diffractometer (LEED), an Auger electron spectroscope (AES) and a device for measuring the surface magneto-optical Faraday effect (SMOFE). *In situ* SMOFE is a suitable approach, in which the probing light can be easily guided from the air to the inside of the UHV chamber. The polarisation of the transmitted light is rotated when the sample is magnetised along the surface plane. (This configuration is called the longitudinal mode.) In a ferromagnetic ultrathin films, the total Faraday rotation angle  $\theta_F$  is proportional to the magnetisation of the material in the region of detection. The theoretical approach for SMOFE measurement is [10]:

$$\theta_F = \rho_F \frac{M_{0z}}{M_s} \frac{L}{\cos\alpha}, \quad (1)$$

where  $\rho_F$  is a Faraday rotatory power which depends on light wavelength, refraction index of material in  $z$ -axis, and magneto-optical constant from internal magnetisation of the material;  $M_{0z}$  is the existing magnetisation in the material and  $M_s$  is the saturation magnetisation of the material;  $L$  is the length of the path along which the light

<sup>a</sup> Present address: 300, Syuefu Road, Chiayi 60004, Taiwan; e-mail: cwsu@mail.ncku.edu.tw

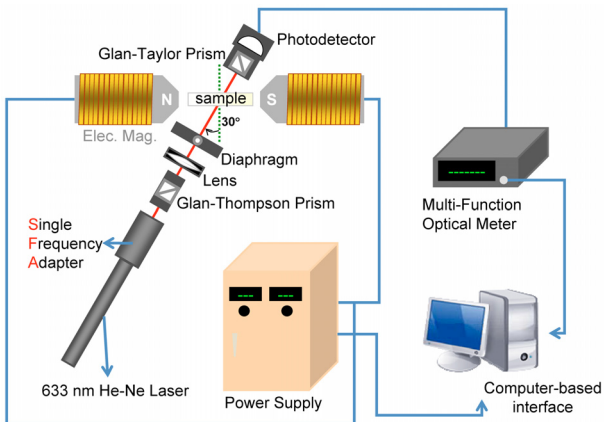


**Fig. 1.** (Color online) The technique of surface magneto-optical Faraday effect exploited in measuring magnetic properties of ultrathin films.

interacts with the magnetic field and  $\alpha$  represents the angle of incidence from the normal to the ZnO surface. The angle  $\alpha$  and  $L$  in this system can be regarded as constants because the angle of incidence in the chamber port is fixed. Figure 1 schematically depicts the SMOFE design.

The wavelength of the probe light from the highly stable polarised He-Ne laser used in SMOFE is 633 nm. A  $p$ -polarised light beam (parallel to incident plane) was focused onto the sample by lens. The photo detector receives only the  $s$ -wave light signal (perpendicular to the optical incidence plane), enabling tiny variations in optical intensities to be observed. The magnetic field can reach 3.2 kOe.

The  $1 \times 1 \times 0.05$  cm<sup>3</sup> commercial ZnO(002) crystal substrate was transparent and polished on both sides. One side was O-terminated and the other side was Zn-terminated when the surface was ordered. Although the O-terminated side was used as substrate in this study, destructive ion sputtering may have destroyed the ordering of the surface. If the top layer of the surface is terminated with oxygen atoms, interesting magnetic interactions are expected because Co/O-ZnO may exhibit unexpected antiferromagnetism. Figure 2 showed the AFM image before transferring the sample into the UHV chamber. The surface is normally covered with dust, impurities, and oxides. To prevent any complications in the ex-situ measurement, the sample had been cleaned ultrasonically by alcohol and acetone. The average height of the sample in the air was around  $1.4 \pm 0.5$  nm. After the ZnO(002) crystal sample was introduced into the UHV chamber, it had to be cleaned by sputtering with Ar<sup>+</sup> at normal incidence (2 keV; target current 10 mA, 30 min) for many hours. A home-made cobalt coil (0.5-mm wire diameter, with a purity of 99.995%) was heated using the thermal-resistive method to evaporate off Co atoms in the UHV chamber. The pressure during the deposition was maintained at around  $1 \times 10^{-9}$  Torr.

### 3 Results and discussion

All measurements were taken at room temperature. After the cleaning process, the surface structure was rougher

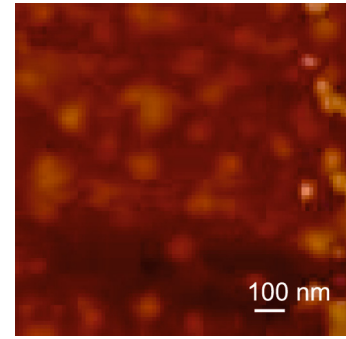


**Fig. 2.** (Color online) The ex situ AFM image of the O-ZnO(002) substrate. The scanning region in this picture is  $1 \mu\text{m}^2$ .

than before. The structure was verified in the absence of a LEED pattern. The growth of the Co film began after cleaning. Figure 3 observed by AES displays typically three-dimensional island growth. The growth of the Co overlayer was monitored by observing the evolution of the Co LMM 771 eV, Zn LMM 985 eV, and O KLL 510 eV peak-to-peak Auger signals. Twenty-five Auger spectra were obtained in 48 h.

The thickness of Co was estimated by the ratio of Co, Zn, and O Auger peak heights using the inelastic-mean-free-path (IMFP) database considering TPP-2M formulae and backscattering factors. The details can be found elsewhere [11,12]. Although the estimate of the thickness is valid only for perfect layer-by-layer growth, local short-range order of the topmost surface layers may have existed. The sputtering process was finished by tuning the ion energy to around 300 eV for 15 min to smooth the surface. The deposition rate was held constant by introducing a stable current in the Co filament. Figure 4 presents  $I_{\text{Co}}/(I_{\text{Zn}} + I_{\text{O}})$  (the ratio of Auger intensities of Co and that of Zn plus O in Fig. 3) versus deposition time. The microstructure Zn-terminated or O-terminated surface is not key to the growth of the covering adsorbate because either surface may be formed before deposition. The ratio in Figure 4 increases and saturates at around 1.4 after 34 h. The adsorbate layer that covers the substrate attenuates the Auger signals. The ratio may saturate when the thickness of the adsorbate exceeds the Inelastic Mean Free Path (IMFP) of the substrate signals. IMFP of Zn is longer than that of O [11]. If the thickness of the Co overlayer exceeds the IMFP of Zn, estimated at 1.97 nm by TPP-2M equation, the Auger signal of Zn attenuates rapidly by a factor of  $1/e$  with adsorbate thickness. The estimated time was used to calibrate the thicknesses of all Co films. Therefore, Co grew at a rate of around 0.06 nm per hour (equivalent to around 0.3 monolayer per hour, ML/h).

The structure of the surface without post-annealing may not exhibit long-range-order. The growth of islands of Co deposited on a sputtered ZnO(002) crystal was as expected. Consequently, the Auger intensity of Co revealed an exponential behaviour in the uptake curve as given in Figure 3. Moreover, variation of the sensitive ratio of Zn/Co Auger intensities depicted in Figure 5 was

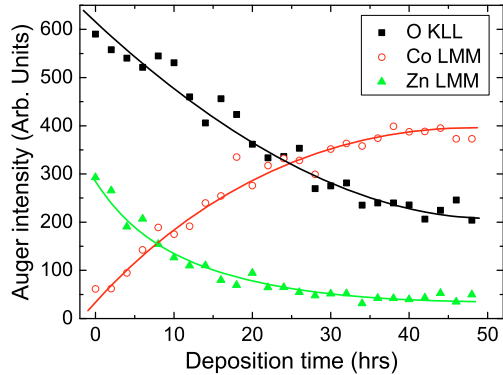


Fig. 3. (Color online) Auger intensities of Co LMM 771 eV, Zn LMM 985 eV, and O KLL 510 eV as Co grows on ZnO(002) bulk. Solid lines are the guides for eyes.

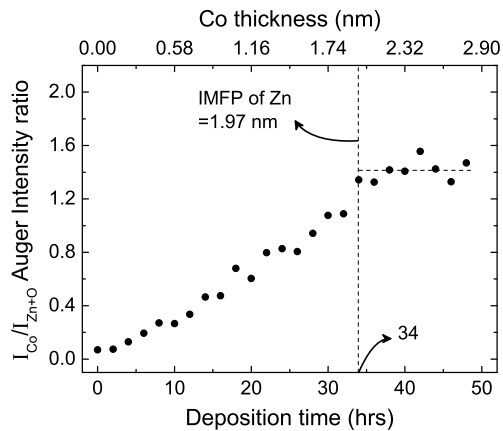


Fig. 4. Auger intensity ratio of  $I_{\text{Co}}/(I_{\text{Zn}} + I_{\text{O}})$  as a function of deposition time. Ratio saturated after 34 h.

used to compare the saturated magnetisation (which is proportional to the Faraday intensity) in the growth of Co. The discontinuous lines in Figure 5 obviously divided the variations into three regions labelled as A, B and C. A simulated surface structure is presented in the top of figure. In the first region, A, the initial structure of the surface, formed by preferential sputtering, is rough and contains many structural defects. In this regime, the adsorbate is grown on the rough surface until almost all of the vacancies are filled with Co atoms. Although Zn/Co Auger intensity ratio declines rapidly with the growth of the adsorbate, Zn signal remains clearly observed up to a thickness of 2.3 ML ( $\sim 0.46$  nm). In region B, the ratio falls gradually because the defects and vacancies in region A have been filled by Co. Further deposition of Co may pseudomorphically stack as like a perfect ZnO substrate structure. Therefore, the Auger intensity ratio may bend at around 2.3 ML. We assume that the turning point, about 2.3 ML, may be the average depth of the surface vacancies. Beyond 7.4 ML, ratio of intensities of the Zn/Co Auger signals saturates because the Co signals fully exceed the detection limit of Zn in region C.

The SMOFE signals increase when the thickness between 2.3 and 4.4 ML. Co grew initially on a flatten surface after region A. In the first half of region B, the growth

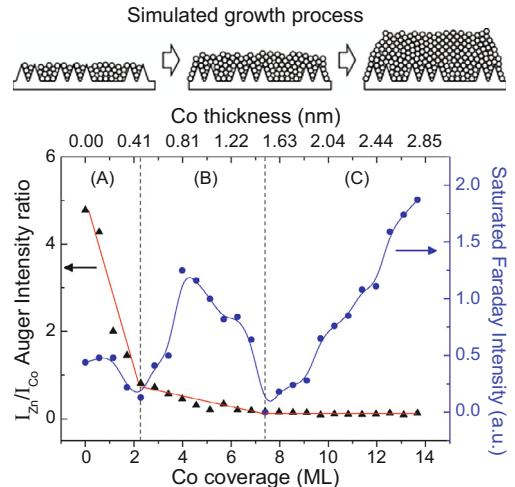
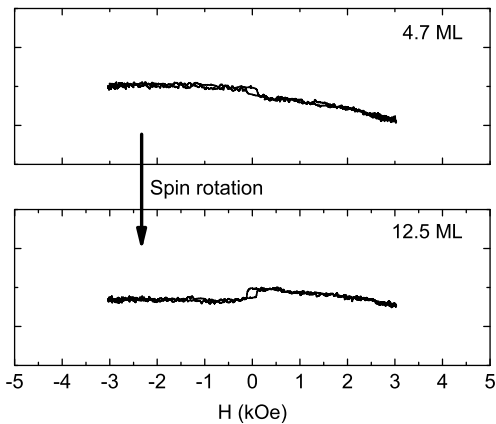
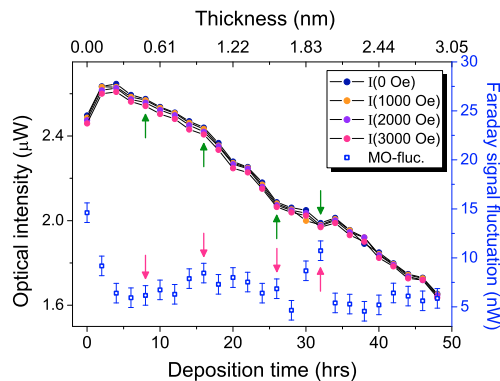


Fig. 5. (Color online) Zn/Co Auger signal ratio as a function of Co coverage is divided, based on assumed growth modes, into regions A, B and C. Relationship between saturated magneto-optical Faraday intensity and Zn/Co ratio in region A demonstrates degree of surface roughness of ZnO.

of Co began to exhibit typical ferromagnetic behaviour. From 4.4 to 7.4 ML, the decrease in SMOFE signal may be caused by the gradual rotation of the easy axis of in-plane magnetisation, such as from left to right, and its interaction with the embedded Co defects. Beyond 7.4 ML, the easy axis of thick Co films may be pinned by the embedded Co close to the interface owing to the dominance of the strong magnetic crystalline anisotropy. The magnetic signal increases monotonically and exhibits ferromagnetic behaviour. When the thickness of Co exceeds 10 ML, the substrate ceases to affect the magnetic interaction. Accordingly, the magnetic signal increases monotonically with thickness. In this investigation, a strong relationship between the magnetic property and the structure of the Co/ZnO system was found. The growth process included two transition points. The surface of the substrate was initially filled with defects and was rough, before it was covered with 2.3 ML of Co. The SMOFE signal is notable when the thickness exceeds 2.3 ML. Therefore, the thickness, which is the depth of surface vacancies of ZnO(002) was to be 2.3 ML ( $\sim 0.46$  nm). The ratio of Auger intensities after 2.3 ML of Co had grown varied as revealed by the varying SMOFE signals. The Co then slowly grew on a flattened surface. The magnetic property exhibits an interesting change at around 7.4 ML (between regions B and C in Fig. 5). The magnetisation reversal in different thickness was found (spin-up state switched to spin-down state). Figure 6 presents the interesting phenomenon of magnetic switching. Two hysteresis loops exhibited spin behaviour at Co thicknesses of around 4.7 and 12.5 ML. Since the measured SMOFE configuration did not vary during the growth of Co, the spin-up to spin-down transition in a hysteresis loop (Fig. 6) may have been caused by the rotation of the in-plane easy axis in the in-plane domain to its reverse direction. Hence, the oscillation of the magnetisation in the growth of thin films, beginning from



**Fig. 6.** The hysteresis loops measured at 4.7 ML and 12.5 ML. Change in thickness between regions B and C reveal change in spin state of magnetic domain.



**Fig. 7.** (Color online) The optical intensity varies with deposition time/calibrated thickness. The intensity  $I$  with growth (scale indicated in the left side) was observed at 0, 1000, 2000, and 3000 Oe field strength. The signal fluctuation in a hysteresis loop (scale indicated in the right side) was also measured. The sensitivity of optical detector is 1 nW (revealed in the error bar).

a Co thickness of 2.3 ML, is attributable to the rotation of the magnetic easy axis in the surface plane.

On the other hand, we analysed the optical intensity at different magnetic fields in the deposition. More Co films covered on the substrate attenuate the transmission intensity. Clearly, the variation of optical intensity versus deposition time/thickness indicated in Figure 7 did not depend on magnetic field. Arrows in Figure 7 indicate significant changes of structural properties during the deposition. These changes are possible for explaining the surface roughness. In the SMOFE measurement, the detection region close to the laser beam has a diameter near 1 mm. All received optical signals reflect the sum of any structural information in this irradiated region. Meanwhile, the fluctuation of the optical signal in a SMOFE hysteresis was also analysed. Figure 7 revealed the Faraday signals fluctuated with the transmission intensities. That means the relationship between the two results with growth was consistent. Although the in situ surface roughness can not be directly accomplished simultaneously in this system, the

method mentioned in this paper may provide an alternative choice in investigating any substance surface in which the initial structure is undetermined.

## 4 Conclusion

In this study, the structural and magnetic properties of a transparent sample Co/ZnO(002) were related and the depth of the surface roughness in a sputtered ZnO(002) substrate was determined. The thickness of Co film was estimated from inelastic-mean-free-paths and by measuring related Auger signal ratios. The variation in surface magneto-optical Faraday intensity is consistent with the growth behaviour and related structural properties. The link between magnetic and structural properties is useful in determining the depth of the surface roughness. Finally, the mean roughness depth of the rough ZnO(002) sample used in the growth of Co films is estimated to be  $2.3 \pm 0.1$  ML ( $0.46 \pm 0.02$  nm).

The authors acknowledged Prof. S.H. Chen's lab in National Chiayi University for scanning the AFM images of samples. The authors would like to appreciate the National Science Council of the Republic of China, Taiwan, for financially supporting this research under Contract Nos. NSC 95-2112-M-415-001, NSC 96-2112-M-415-005-MY2, 98-2112-M-415-003-MY3, and National Chiayi University academic project under No. NCUY 96T001-06-04-003. Ted Knoy is appreciated for his editorial assistance.

## References

1. C.S. Shern, J.S. Tsay, H.Y. Her, Y.E. Wu, R.H. Chen, *Surf. Sci.* **429**, 497 (1999)
2. Y.E. Wu, C.W. Su, C.S. Shern, M.T. Lin, *Chin. J. Phys.* **39**, 182 (2001)
3. N.W.E. McGee, M.T. Johnson, J.J. de Vries, J. aan de Stegge, *J. Appl. Phys.* **73**, 3418 (1992)
4. C.W. Su, J.S. Tsay, C.H. Hwang, Y.D. Yao, *J. Appl. Phys.* **97**, 10J111 (2005)
5. J.S. Tsay, Y.D. Tao, K.C. Wang, W.C. Gheng, C.S. Yang, *Surf. Sci.* **507–510**, 498 (2002)
6. Y. Matsumoto, M. Murakami, T. Shono, T. Hasegawa, T. Fukumura, M. Kawasaki, P. Ahmet, T. Chikyow, S.Y. Koshihara, H. Koinuma, *Science* **291**, 584 (2001)
7. Y.L. Soo, G. Kioseoglou, S. Kim, Y.H. Kao, P.S. Devi, J. Parise, R.J. Gambino, P.I. Gouma, *Appl. Phys. Lett.* **81**, 655 (2002)
8. C.M. Wang, V. Shutthanandan, S. Thevuthasan, T. Droubay, S.A. Chambers, *J. Appl. Phys.* **97**, 073502 (2005)
9. N. Akdogan, A. Nefedov, A. Westphalen, H. Zabel, R.I. Khaibullin, L.R. Tagirov, *Superlatt. Microstruct.* **41**, 132 (2007)
10. J.M. Liu, *Photonics Devices* (Cambridge University Press, Cambridge, 2005), p. 299
11. C.J. Powell, A. Jablonski, NIST Electron Inelastic-Mean-Free-Path Database Version 1.1 (National Institute of Standards and Technology, Gaithersburg, MD, 2000)
12. C.W. Su, H.Y. Ho, C.S. Shern, R.H. Chen, *Thin Solid Films* **425**, 139 (2002)